Математички Билтен
49 (LXXV) 2 (2025), 75–95

UDC: [517.912:517.524:[519.71:517.938]
DOI: 10.37560/matbil2549275ql

DELAYED-FEEDBACK STABILIZATION OF EQUILIBRIA IN THE FRACTIONAL-ORDER RÖSSLER AND LORENZ SYSTEMS: A COMPARATIVE ANALYSIS

FERIDE QORROLLI LUBISHTANI [1], GJORGJI MARKOSKI [2],
AND ALEKSANDAR GJURCHINOVSKI [2]

Abstract. This study investigates the stabilisation of equilibria in Rössler and Lorenz systems incorporating time-delayed feedback control (TDFC) with delay parameter τ and feedback gain K. The research identifies combinations of feedback gain and delay that stabilize the system's equilibria through two complementary approaches: a local spectral test based on the characteristic equation and Matignon's criterion, and direct simulation using a fractional forward Euler of Grünwald-Letnikov type. Stabilization in simulations is certified by requiring all trajectories to satisfy a finite-time tolerance 10^{-2}, $\forall\, t \geq 200$. The results indicate that TDFC can suppress chaotic dynamics where present and/or enforce convergence to the target equilibrium: The Rössler system exhibits two disjoint stability islands and 19.5% contraction between theoretical and numerical stability sets, whereas the Lorenz system shows full-domain stability with 100% agreement; this contrast is traced to a tenfold difference in the oscillation frequency of the unstable eigenvalues. The framework developed here is intended as a template for subsequent studies of other Lorenz-type systems.

1. INTRODUCTION

Fractional-order differential models effectively capture the memory effects in various physical, biological, and engineering processes, demonstrating greater suitability than classical models in describing anomalous diffusion and similar phenomena [1], [2], [3], [4], [5]. When time delays are added to these models to represent reaction times, transport delays, or discretely implemented feedback, one obtains fractional delay differential equations in which long-term memory and delay coexist; fractional delay versions of Rössler and Lorenz-type systems

2010 *Mathematics Subject Classification.* Primary 34K37; Secondary 34K20, 34K35, 93D15, 37M05.
Key words and phrases. Fractional-order systems with delay, Rössler system, Lorenz system, Delayed feedback control.

provide concrete examples of such dynamics, exhibiting multistability, complex bifurcations, and chaotic attractors [6], [7], [8].

Three-dimensional Lorenz-type systems are essential models for exploring chaos and control, with the classical Lorenz system [9] and the simpler Rössler system [10] serving as key mathematical frameworks for studying bifurcations, chaotic attractors, and equilibrium stabilization. In the last few decades, the Lorenz-type system has grown to include Chen, Lü, Yang, Liu, Shimizu–Morioka, Burke–Shaw, and other Lorenz-type systems [6]. Numerous studies have addressed fractional versions of these systems, with or without delay, including the existence of chaos, bifurcations, stability, controllability, and control design [8], [11], [12], [13]. However, existing works (to our knowledge) usually focus on a single system and rarely provide a comprehensive comparative analysis of stabilization with control over feedback and delay parameters.

Time-Delayed Feedback Control (TDFC), introduced by Pyragas in 1992, is a key method for stabilizing chaotic systems. TDFC adds a feedback term of the form $K(y(t-\tau)-y(t))$, where K is the feedback gain, and τ is the time delay, with specified ranges [14].

This article represents the first part of a broader study on delayed-feedback stabilization in fractional-order chaotic systems. We study the fractional Rössler and Lorenz systems with common order $\alpha = 0.9$, using a scalar TDFC term in the second equation. The common value $\alpha = 0.9$ is used as a representative fractional order below unity, allowing both systems to be compared under the same memory effect. In this way, the differences observed in the stability regions can be related mainly to the spectral and structural properties of the two systems, rather than to different fractional orders. For classical parameter sets, we analyze the stabilization of a representative unstable equilibrium and assess whether the same TDFC can suppress chaotic dynamics where present and/or enforce convergence, and why its effectiveness ranges from wide, robust domains to narrow stability "islands" depending on spectral and structural properties.

The main contribution of this paper is a systematic comparative analysis of time-delayed feedback control (TDFC) in fractional-order Rössler and Lorenz systems with $\alpha = 0.9$, using a unified theoretical-numerical framework. We derive stability regions in the (τ, K)-plane from the characteristic equation and Matignon's criterion [15], [7], verify them via a fractional Forward Euler–Grünwald–Letnikov scheme (chosen for its simple implementation and favorable stability and computational efficiency- see [8]), and quantify the theory-numeric agreement (80.5% for Rössler, 100% for Lorenz). We further provide an interpretation of these regions in terms of eigenvalue spectra and oscillation frequencies.

We establish a basic comparative framework that, in subsequent papers, will be extended to the Chen, Lü, Yang, Liu, Shimizu–Morioka, and Burke–Shaw systems, allowing a broader comparative analysis of the Lorenz–type family in the fractional regime with TDFC.

All analytical and numerical results reported here are obtained from the software Mathematica 14.3.

2. BACKGROUND

There are several approaches for fractional-order operators; however, for the purposes of this study, we only consider the Caputo and Grünwald-Letnikov meanings.

Definition 2.1. [1],[16] The (left) Caputo fractional derivative is defined as:

$$ {}^{C}D^{\alpha} f(t) = \frac{1}{\Gamma(n-\alpha)} \int_a^t (t-\tau)^{n-\alpha-1} f^{(n)}(\tau)\, d\tau \tag{2.1} $$

where $n = \lceil \alpha \rceil$ (n is the smallest integer greater than α), $\Gamma(\cdot)$ is the gamma function (see [3]), and a is the lower limit of the integral.

Definition 2.2. [1],[16] The (left) Grünwald-Letnikov definition is a generalization of the traditional derivative. It is defined as:

$$ {}^{GL}D^{\alpha} f(t) = \lim_{h \to 0} \frac{1}{h^{\alpha}} \sum_{k=0}^{\left\lfloor \frac{t-a}{h} \right\rfloor} (-1)^k \binom{\alpha}{k} f(t-kh), \tag{2.2} $$

where α is the order of the derivative, h is the step size, and $\binom{\alpha}{k}$ is the binomial coefficient of the form $\binom{\alpha}{k} = \frac{\Gamma(\alpha+1)}{\Gamma(k+1)\Gamma(\alpha-k+1)}$.

3. ANALYSIS OF FRACTIONAL ORDER SYSTEMS WITH DELAY (FDDE)

3.1. **General form and stability analysis of FDDEs.** We examine the effect of delays on the Lorenz-type systems presented in Petra's paper [4],[6], and Rössler system here we modify by adding delays to the systems in the general form as follows [7]:

$$ {}^{C}D_t^{\alpha_i} x_i(t) = f_i\big(t, x_1(t), x_2(t), \ldots, x_n(t)\big) + F_i(t), \quad i = 1, 2, \ldots, n, \tag{3.1} $$

$$ F_i(t) = \sum_{j=1}^{n} K_{ij}\big[x_j(t-\tau) - x_j(t)\big] \tag{3.2} $$

where $F_i(t)$ is the delayed feedback force applied to the i-th component of the system, K_{ij} are the gain factors of the feedback terms, τ is the constant delay, f_i are nonlinear functions, and $x_i(0) = c_i$ are initial conditions. The vector representation of initial conditions is:

$$ D^{\mathbf{ff}}\mathbf{x} = \mathbf{f}(\mathbf{x}), \tag{3.3} $$

where $\mathbf{ff} = [\alpha_1, \alpha_2, ..., \alpha_n]^T$ for $0 < \alpha_i < 2, (i = 1, 2, ..., n)$ and $\mathbf{x} \in \mathbb{R}^n$. The equilibrium points of the system (3.4) can be calculated as follows:

$$ \mathbf{f}(\mathbf{x}) = 0 \tag{3.4} $$

and we further assume that it $E^* = (x_1^*, x_2^*, ..., x_n^*)$ is the equilibrium point of the system (3.3). The Jacobian matrix $\mathbf{J}$ at the equilibrium point E^* is the same for fractional systems as it is for integer-order systems because linearization depends only on the system equations and not on the order of the derivatives.

We suppose that the equilibrium point E^* is unstable. To stabilize it, we used the delayed feedback control (3.2), as per Gjurchinovski's research (see [7]).

Theorem 1. *The equilibrium point E^* of the system* (3.1) *and* (3.2) *is locally asymptotically stable if and only if all the roots s of the characteristic equation:*

$$\det[\Delta(s)] = 0 \tag{3.5}$$

have negative real parts, that is,

$$|\arg(s)| > \frac{\pi}{2} \tag{3.6}$$

The matrix $\Delta(s)$ is given by the following equation and its components $a_{ij} = \left(\frac{\partial f_i}{\partial x_j}\right)$ are evaluated at the equilibrium point E^*.

$$\Delta(s) = \begin{pmatrix} s^{\alpha_1} - a_{11} + K_{11}(1-e^{-sT}) & -a_{12} + K_{12}(1-e^{-sT}) & \cdots & -a_{1n} + K_{1n}(1-e^{-sT}) \\ -a_{21} + K_{21}(1-e^{-sT}) & s^{\alpha_2} - a_{22} + K_{22}(1-e^{-sT}) & \cdots & -a_{2n} + K_{2n}(1-e^{-sT}) \\ \vdots & \vdots & \ddots & \vdots \\ -a_{n1} + K_{n1}(1-e^{-sT}) & -a_{n2} + K_{n2}(1-e^{-sT}) & \cdots & s^{\alpha_n} - a_{nn} + K_{nn}(1-e^{-sT}) \end{pmatrix} \tag{3.7}$$

Remark 3.1: Special case when $\alpha_1 = \alpha_2 = ... = \alpha_n = \alpha$, the characteristic equation is:

$$\det\left(\lambda \mathbf{I} - \mathbf{J}\right) = 0 \tag{3.8}$$

which is a polynomial of degree n in λ, where $\lambda = s^{\alpha}$. In this case, the stability condition (3.6) is:

$$|\arg(\lambda)| > \alpha \frac{\pi}{2} \tag{3.9}$$

For a complex number z, $\Re(z)$ and $\Im(z)$ denote its real and imaginary parts, respectively.

Throughout this paper, we consider fractional-order systems with equal orders $\alpha_1 = \alpha_2 = ... = \alpha_n = 0.9$, corresponding to the special case in Remark 3.1. For such systems, the Matignon criterion (3.9) becomes $|\arg(\lambda)| > 0.45\pi \approx 1.414 rad$. Since $\alpha = 0.9$ is close to unity, this sectorial condition is numerically verified by checking $\Re(\lambda) < 0$ for all eigenvalues λ, which is computationally efficient and equivalent for the parameter regimes studied.

In the case where the system is stable (unstable), all its deviations are directed toward the equilibrium point over time, whereas in the second case, these deviations diverge from the equilibrium point, causing instability. Whereas, in the case where we have these deviations combined, chaos is caused [17].

In a 3D nonlinear dynamical system, a *saddle point* is an equilibrium point if the equivalent linearized model has eigenvalues in both stable and unstable areas. If one eigenvalue is unstable while the others are stable, the saddle point is called a saddle point of index 1. A saddle point of index 2 has one stable and two unstable eigenvalues. Keeping the eigenvalue λ in the unstable area is a necessary condition for the fractional system (3.3) to remain chaotic [18]:

$$\tan\left(\alpha \frac{\pi}{2}\right) > \frac{|\Im(\lambda)|}{\Re(\lambda)} \implies \alpha > \frac{2}{\pi} \tan^{-1}\left(\frac{|\Im(\lambda)|}{\Re(\lambda)}\right) =: \alpha_{crit} \tag{3.10}$$

Theorem 2. *(Odd number limitation)* [19]. *Let E be an unstable equilibrium point of the fractional-order system* (3.1) *in the absence of control ($K_{ij} = 0$), and* **J** *the corresponding Jacobian matrix at E. If* **J** *has an odd number of positive real eigenvalues, then the time-delay feedback control* (3.2) *cannot stabilize the unstable equilibrium E for any values of the control parameters K_{ij} and τ.*

3.1.1. *Analytical analysis through the characteristic equation.* After computing the equilibrium points and determining whether they can be stabilized or not (according to the condition of Theorem 2), for each pair (τ, K) from a given parametric network, we: define the complex function; choose a suitable window in the complex plane s, with real and imaginary parts in bounded intervals; use a scheme (in Mathematica FindRoot) with multiple starting points inside this window to find all numerically visible roots of the characteristic equation; and eliminate repeated roots using a small tolerance criterion.

Based on this approximate spectrum, the parameter pair (τ, K) is classified as stabilizing for equilibrium E^* if all computed characteristic roots s satisfy the sectorial stability condition (3.6) (equivalently, $\Re(s) < 0$ for all roots). For the commensurate case considered in this study ($\alpha_1 = \alpha_2 = \cdots = \alpha_n = 0.9$, Remark 3.1), it is convenient to introduce the transformed roots $\lambda = s^\alpha$, in which case the fractional sector condition becomes $|\arg(\lambda)| > \alpha\pi/2 = 0.45\pi$. In the computations we enforce this fractional sector test directly; since α is close to unity, we also monitor $\Re(\lambda) < 0$ as a convenient auxiliary proxy, which agrees with the sector classification over the scanned parameter ranges. The theoretical stability regions in the (τ, K) plane are then obtained by labeling each grid point as stable or unstable according to these criteria.

3.1.2. *Numerical method and verification.* To verify the results obtained from the analysis based on the characteristic equation, we perform direct numerical simulations of the fractional-order systems with delay. Unlike Gjurchinovski et al. (2010), where a fractional Adams-type method was employed, we use a fractional forward Euler method (FEM) of Grünwald-Letnikov type,which is simpler and easier [8] to implement and naturally fits with the discrete structure of the delayed feedback term. In a previous paper [20], we compared several fractional numerical methods for delayed differential equations. The results show that the Forward Adams Method (FAM) and FEM have smaller relative errors. The FEM Grünwald-Letnikov scheme is first-order accurate in time with a local truncation error of order $O(h^\alpha)$, which is adequate for stability classification but not intended for high-precision trajectory computation. However, due to the complexity and high computational cost of FAM, we favor FEM as a good solution for simplicity of implementation and the accuracy needed to construct stability maps in the (τ, K) plane.

For a scalar component $y(t)$ and order $\alpha \in (0, 1)$, we consider a uniform time grid $t_n = nh$ ($n = 0, 1, \ldots, N$) with step size $h > 0$ and denote $y_n \equiv y(t_n)$. We employ a Grünwald-Letnikov-type approximation (used in the fractional forward

Euler scheme), with coefficients

$$c_j^{(\alpha)} = (-1)^{j-1}\binom{\alpha}{j}, \qquad j \geq 1,$$

so that the fractional "memory" term at step n is expressed in terms of past samples.

In vector form, for a system written as follows:

$${}^{C}D_t^{\alpha} x(t) = f\big(t, x(t), x(t-\tau)\big),$$

(in our models, the delayed argument enters only through the y-component), the corresponding time-discrete update with step size h can be written as follows:

$$x_{n+1} = \sum_{j=1}^{n} c_j^{(\alpha)}\, x_{n+1-j} + h^{\alpha} f\big(t_n, x_n, x_{n-m}\big), \qquad m = \left\lfloor \frac{\tau}{h} \right\rfloor,$$

(consistent with the update form used in our implementation).
Discretization of the delay term. In the present study, the delay appears only in the second equation (the y-component) through the TDFC term. Therefore, on the grid $t_n = nh$, the delayed value is evaluated using a memory buffer (nearest-node) approximation:

$$y(t_n - \tau) \approx y_{n-m}$$

For $t_n < \tau$ (i.e., $n < m$), a history function on $[-\tau, 0]$ is required; here, we adopt a constant history $y(t) \equiv y_0$ (equivalently, $y_n \equiv y_0$ for $n < m$). In the parameter sweep, τ is chosen on a grid compatible with h, hence the nearest-node evaluation is exact on the discrete mesh.

In the implementation, the coefficients $c_j^{(\alpha)}$ are precomputed once up to the final integration time t_{final} and reused for all pairs (τ, K), which reduces the numerical cost of the fractional "long memory". The system is integrated with time step h up to t_{final}, starting from initial conditions in the chaotic regime (the same for all (τ, K)), while the delay is initially switched off during the transient interval $[0, mh]$ so that the history buffer is filled. In all simulations, we use $h = 0.005$ and $t_{\text{final}} = 300$. Comparing the number of stable points for different values of the time step ($h = 0.01, h = 0.005, h = 0.004, h = 0.0025$), we obtain an average of about 2137 stable points; the values $h = 0.005$ gives 2133 points, a very small deviation from the average. Thus, we choose this step as a good compromise between numerical accuracy and computational cost.

To construct the numerical stability map, for each pair (τ, K) in the parametric network: We integrate the fractional system with the Euler-GL scheme from $t = 0$ to $t = t_{\text{final}}$, including the TDFC control terms in the discrete component equations of the corresponding components; We choose a time t_{check} large enough to overcome transients (e.g. $t_{\text{check}} = 200$) and estimate the maximum deviation of the discrete trajectory from the target equilibrium $E^* = (x^*, y^*, z^*)$:

$$\delta(\tau, K) = \max\{|x(t) - x^*|,\ |y(t) - y^*|,\ |z(t) - z^*|\}$$

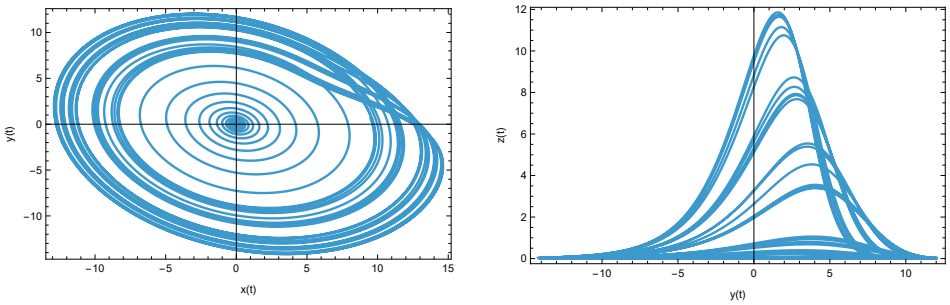


FIGURE 1. Fractional order Rössler system without delays, for $a = 0.4$, $b = 0.2$, $c = 10$, $\alpha = 0.9$ and initial conditions $x(0) = 0.2, y(0) = 0.48, z(0) = 0.731$.

We fix a threshold $\varepsilon = 10^{-2} > 0$ and classify the pair (τ, K) as numerically stable if $\delta(\tau, K) \leq \varepsilon$, and as unstable otherwise. The above tolerance-based classification is a *practical, finite-time* stability criterion: it declares (τ, K) stable when the computed trajectory remains within the prescribed tolerance ε of the target equilibrium for $t \geq t_{\text{check}}$, i.e., over the simulated window $[t_{\text{check}}, t_{\text{final}}]$. This test is used as a numerical proxy for asymptotic stability; however, it *approximates* and is *not strictly equivalent* to asymptotic stability as $t \to \infty$. Accordingly, the reported stability maps should be interpreted as numerically verified stability regions under the chosen discretization, tolerance, and finite simulation horizon.

Thus, all pairs (τ, K) that satisfy the above criterion are shown in black in the (τ, K) plane, whereas the others are left white, forming the numerical stability maps.

3.2. **Numerical example.**

This part of the paper is perhaps the most important because here we present the behavior of fractional-order systems with added delays: the **Rössler** system and the **Lorenz** system.

3.2.1. ***Fractional order Rössler system with delay.*** The fractional-order Rössler system with delay is described as follows:

$$\begin{aligned} {}^0D_t^{\alpha} x(t) &= -y(t) - z(t), \\ {}^0D_t^{\alpha} y(t) &= x(t) + ay(t) + K(y(t-\tau) - y(t)), \\ {}^0D_t^{\alpha} z(t) &= z(t)[x(t) - c] + b, \end{aligned} \tag{3.11}$$

where the fractional order of the derivative α is 0.9, K is the gain factor of the feedback terms, τ is the delay, and the parameters are $a = 0.4$, $b = 0.2$, and $c = 10$.

For $K = 0$, the system (3.11) exhibits chaotic behavior, as shown in Figure 1.

As we know, equilibrium points are determined in the same way for systems with integer order derivatives and for those with fractional order derivatives, since they are obtained by solving $f(x, y, z) = 0$; then the Rössler system of fractional order (without control) has two equilibrium points, E_+ and E_-. Solving $f(x, y, z) = 0$ gives two equilibria with coordinates $(x_\pm, y_\pm, z_\pm)$ as follows:

$$x_\pm = \frac{c}{2}\left(1 \pm \sqrt{1 - \frac{4ab}{c^2}}\right),$$
$$y_\pm = -\frac{c}{2a}\left(1 \pm \sqrt{1 - \frac{4ab}{c^2}}\right),$$
$$z_\pm = \frac{c}{2a}\left(1 \pm \sqrt{1 - \frac{4ab}{c^2}}\right).$$

for $(a, b, c) = (0.4, 0.2, 10)$, we obtain numerically: $E+ = (9.9919, -24.98, 24.98)$ and $E_- = (0.008, -0.02, 0.02)$. From the Jacobian matrix:

$$\mathbf{J} = \begin{pmatrix} 0 & -1 & -1 \\ 1 & a & 0 \\ z^* & 0 & x^* - c \end{pmatrix}. \tag{3.12}$$

and equation (3.7) we have:

$$\lambda^3 + \lambda^2(c - x^* - a) + \lambda(ax^* - ac + z^* + 1) + (c - x^* - az^*) = 0$$

Substituting the values of the parameters a, b, and c, we have:

$$\lambda^3 + \lambda^2(9.6 - x^*) + \lambda(0.4x^* + z^* - 3) + (10 - x^* - 0.4z^*) = 0$$

Lastly, from the last equation for each equilibrium point E_+ and E_-, we have: $\lambda_{1,2} = 0.0038 \pm 5.09645i, \lambda_3 = 0.3844 + 0i$ and $\lambda_1 = -9.9900 + 0i, \lambda_{2,3} = 0.1990 \pm 0.9797i$, respectively. As shown in Gjurchinovski et al. [7] and in accordance with Remark 3.1, we apply the Matignon stability condition (3.9) to each eigenvalue, from where both equilibrium points are unstable. For equilibrium point E_+, we have: $|\arg(\lambda_{1,2})| \approx 1.570\,\text{rad} > 1.414$ (*lies inside the fractional stability sector*), and $|\arg(\lambda_3)| = 0 < 1.414$ (*violates Matignon's condition*). Although the complex pair $\lambda_{1,2}$ satisfies the sectorial condition, the real eigenvalue λ_3 violates the Matignon criterion, rendering E_+ unstable specifically, a saddle point of index 1 (two stable directions from the complex pair, one unstable direction from $\lambda_3 > 0$). Since the Jacobian at E_+ (evaluated for the uncontrolled system, $K = 0$) has an odd number of eigenvalues with positive real parts, based on Theorem 2, the time-delayed feedback control cannot stabilize this point. We therefore exclude E_+ from the TDFC analysis.

Similarly, for equilibrium point E_- we have: $|\arg(\lambda_1)| = \pi \approx 3.14\,\text{rad} > 1.414$, (satisfies condition (3.9)), and $|\arg(\lambda_{2,3})| = \arctan(0.980/0.199) \approx 1.373\,\text{rad} < 1.414$, (not satisfies condition (3.9)). The complex pair violates the Matignon criterion, rendering E_- unstable a saddle point of index 2. Since E_- has two positive real eigenvalues (the complex pair $\lambda_{2,3}$), an even number than by Theorem

3.2, TDFC can stabilize E_- for appropriate (τ, K). The stabilization domain is determined in the following sections.

Linearization around the equilibrium point $E^* = (x^*, y^*, z^*)$ is given by the following system:

$$\begin{aligned} {}^0D_t^\alpha \tilde{x}(t) &= -\tilde{y}(t) - \tilde{z}(t) \\ {}^0D_t^\alpha \tilde{y}(t) &= \tilde{x}(t) + a\tilde{y}(t) + K\left[\tilde{y}(t-\tau) - \tilde{y}(t)\right] \\ {}^0D_t^\alpha \tilde{z}(t) &= z^*\tilde{x}(t) + x^*\tilde{z}(t) - c\tilde{z}(t) \end{aligned} \tag{3.13}$$

derived from $x(t) = x^* + \tilde{x}(t)$, $y(t) = y^* + \tilde{y}(t)$, and $z(t) = z^* + \tilde{z}(t)$. Here, $\tilde{x}(t)$, $\tilde{y}(t)$, and $\tilde{z}(t)$ are small perturbations around the equilibrium point. The linearization is obtained by substituting these expressions into (3.11), expanding to the first order, and using the equilibrium conditions $-y^* - z^* = 0, x^* + ay^* = 0$, and $b + z^*x^* - cz^* = 0$ to eliminate all constant terms. The system (3.13) can be written in matrix form, as follows:

$$\begin{pmatrix} D_*^\alpha \tilde{x}(t) \\ D_*^\alpha \tilde{y}(t) \\ D_*^\alpha \tilde{z}(t) \end{pmatrix} = \mathbf{J} \cdot \begin{pmatrix} \tilde{x}(t) \\ \tilde{y}(t) \\ \tilde{z}(t) \end{pmatrix} + K \begin{pmatrix} 0 \\ \tilde{y}(t-\tau) - \tilde{y}(t) \\ 0 \end{pmatrix} \tag{3.14}$$

where $\mathbf{J}$ is the Jacobian matrix. Furthermore, the characteristic equation is $\det[\Delta(s)] = 0$, and

$$\Delta(s) = \begin{pmatrix} s^\alpha & 1 & 1 \\ -1 & s^\alpha - a + K(1 - e^{-s\tau}) & 0 \\ -z^* & 0 & s^\alpha - (x^* - c) \end{pmatrix} \tag{3.15}$$

Since the unstable equilibrium point E_- can be stabilized by TDFC, from figure 2 the plot of parameter pairs (τ, K), with delay $\tau \in [0, 12]$ on the horizontal axis and feedback gain $K \in [0, 6]$ on the vertical axis, for which the real part of each root is negative. The shaded regions correspond to the local asymptotic stability of E_-, whereas the unshaded part of the plane corresponds to instability. Two disjoint stability domains are visible. The first, a tall block for small delays, covers a wide interval of gain range and extends from $\tau = 0$ up to approximately $\tau \approx 4$, indicating that for short delays the equilibrium can be stabilized for nearly any moderate gain. The second, much narrower domain appears for larger delays, $\tau \approx$ 8–11, and is confined to an intermediate band of gains, reflecting that stabilization is again possible at long delays but only for a restricted range of K. Between these two shaded regions, for intermediate delays $\tau \approx$ 4–8, no stable points are found for any gain in the considered interval, evidencing a delay-induced loss of stability that cannot be compensated by changing K. This non-monotone dependence on τ is inherent to delay feedback systems: the characteristic equation contains exponential terms $e^{-s\tau}$ and is therefore transcendental with infinitely many characteristic roots. As τ increases, additional branches of roots become relevant and may cross the stability boundary. Thus, stability cannot, in general, be preserved for arbitrarily large delays simply by increasing K. Consequently, the stabilization set typically splits into bounded "stability

islands" in the (τ, K)-plane, highlighting the strong sensitivity of TDFC performance to the choice of (τ, K). The overall two-island structure suggests that, in the fractional Rössler system, time-delayed feedback control is highly sensitive to the choice of delay and gain and admits only two separated windows of successful stabilization in the (τ, K)-plane, which is consistent with the transcendental nature of the characteristic equation and the appearance of infinitely many roots as τ increases.

The spectral mechanism behind this two-island structure is discussed in Section 4.

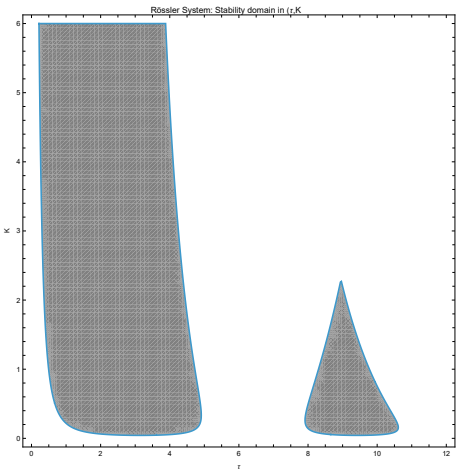


FIGURE 2. Fractional Rössler system: local stability of E_- via characteristic equation: shaded area = stable $K \in [0, 6]$ and $\tau \in [0, 12]$.

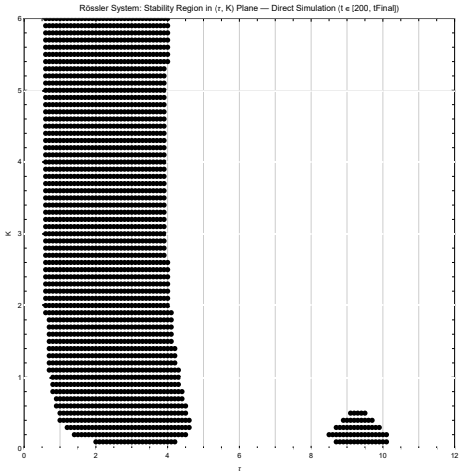


FIGURE 3. Rössler system (fractional $\alpha = 0.9$) with TDFC: black dots mark (τ, K) stable for $t \geq 200$ with tolerance 10^{-2} under direct simulation.

To confirm the stabilization, we performed a numerical simulation using the forward fractional Euler method of Grünwald-Letnikov type on the system (3.11) with the delay included, as shown in the results in the following figures 3, 4 and 5. The Figure 3 shows the stability region in the (τ, K)-plane: each black dot marks a delay-gain pair for which a long-time simulation of the fractional system drives the state to the target equilibrium E_- and keeps it within a tolerance of 10^{-2} on the interval $t \in [200, 300]$; the dots form two separated clusters corresponding to the small delay and large delay stability islands predicted by the characteristic equation (with a small difference which will be analyzed in the discussion section). We selected the stable pair $(\tau, K) = (0.6, 1.9)$ from the left island and displayed it in Figures 4 and 5. In Figure 4 the time series of $x(t)$, $y(t)$, and $z(t)$ start with sizable oscillations, but these decay monotonically. After a transient of order $t \approx 200$, each component settles near a constant value equal to the corresponding coordinate of E_-, consistent with asymptotic stabilization in the time domain. Figure 5 shows the same solution in the three-dimensional phase

space: the trajectory initially traces large outer loops reminiscent of the uncontrolled chaotic attractor, then spirals inward along increasingly tight turns and ultimately collapses into a small neighborhood of E_-. Taken together, Figures 3-5 demonstrate not only where TDFC succeeds in the (τ, K)-plane but also how it suppresses the chaotic motion and produces a stable fixed point in both numerical and geometric terms.

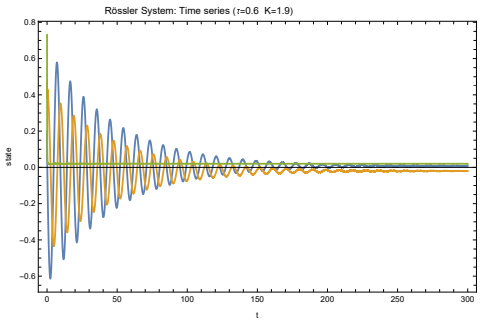


FIGURE 4. The time series plot illustrates the progression of $x(t)$ (blue line), $y(t)$ (orange line), and $z(t)$ (green line) within the fractional-order Rössler system.

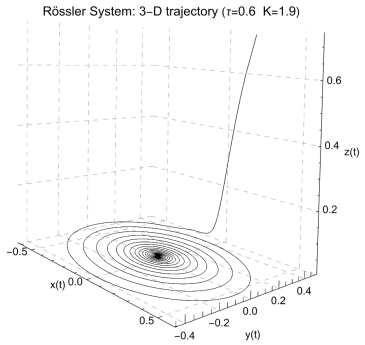


FIGURE 5. The 3D graph of $x(t)$, $y(t)$, and $z(t)$ displays the path of the system converging to a stable area. Time evolves from the outer loops toward the centre.

3.2.2. ***Fractional order Lorenz system with delay***. The fractional-order Lorenz system with delay is described as follows:

$$\begin{aligned} {}^0D_t^{\alpha} x(t) &= a\,[y(t) - x(t)]\,, \\ {}^0D_t^{\alpha} y(t) &= x(t)(c - z(t)) - y(t) + K\,[y(t-\tau) - y(t)]\,, \\ {}^0D_t^{\alpha} z(t) &= x(t)y(t) - bz(t), \end{aligned} \tag{3.16}$$

where the fractional order of the derivative α is 0.9, K is the gain factor of the feedback terms, τ is the delay, and the parameters are $a = 10$, $b = 8/3$, and $c = 28$.

The equilibria in the Lorenz system of fractional order with delays are the same as those of the system without delays, so there are three equilibria, E_0, E_+, and E_-. The first equilibrium is independent of the parameters: $a = 10$, $b = 8/3$, and $c = 28$ and is located at the origin $E_0 = (0, 0, 0)$. The last two symmetric equilibria are dependent on the values of these parameters and from formulas:

$$x = \pm\sqrt{b(c-1)}, \quad y = \pm\sqrt{b(c-1)}, \quad z = c - 1.$$

obtain $E_+ = (6\sqrt{2}, 6\sqrt{2}, 27)$ and $E_- = (-6\sqrt{2}, -6\sqrt{2}, 27)$. For these equilibria, we calculate the eigenvalues from the Jacobian matrix:

$$\mathbf{J} = \begin{pmatrix} -a & a & 0 \\ c - z^* & -1 & -x^* \\ y^* & x^* & -b \end{pmatrix} \tag{3.17}$$

and equation (3.7) we have:

$$\lambda^3 + \lambda^2(1 + a + b) + \lambda(a + b + ab - ac - (x^*)^2 + az^*) + \\ + (ab - abc + ax^*y^* + abz^* - a(x^*)^2) = 0$$

Substituting the values of the parameters a, b, and c, we have:

$$\lambda^3 + \frac{41}{3}\lambda^2 + \lambda(-\frac{722}{3} - (x^*)^2 + 10z^*) + (720 + 10x^*y^* + \frac{80}{3}z^* - 10(x^*)^2) = 0$$

Lastly, from the last equation for each equilibrium point, we obtain: E_0 with eigenvalues $\lambda_1 = -22.8277, \lambda_2 = 11.8277$, and $\lambda_3 = -2.6667$, whereas the eigenvalues of E_+ and E_- are $\lambda_1 = -13.8546$, and $\lambda_{2,3} = 0.09396 \pm 10.1945i$. Then, each eigenvalue is tested to see if it satisfies the Matignon condition (3.9), or not. So, for the equilibrium point E_0 we have: $|\arg(\lambda_1)| = \pi > 1.414$ rad, $|\arg(\lambda_2)| = 0 < 1.414$ rad, and $|\arg(\lambda_3)| = \pi > 1.414$ rad. Here, we can see that the positive real eigenvalue λ_2 violates the Matignon criterion, rendering E_0 unstable. Since E_0 (evaluated for the uncontrolled system, $K = 0$) has one positive real eigenvalue (odd number), then Theorem 2 precludes stabilization by TDFC. Consequently, we exclude E_0 from further analysis.
For E_+ at $\alpha = 0.9$, we apply the Matignon condition to each eigenvalue: $|\arg(\lambda_1)| = \pi > 1.414$ rad, $|\arg(\lambda_{2,3})| \approx 1.561$rad > 1.414 rad. All eigenvalues satisfy the Matignon criterion (3.9), hence E_+ (and by symmetry E_-) are locally stable for the fractional Lorenz system at $\alpha = 0.9$ even without control $(K = 0)$, as confirmed in Figure 3.4.

For the complex pair $\lambda_{2,3} = 0.09396 \pm 10.1945i$, from (3.10), the critical fractional order above which instability emerges is $\alpha_{\text{crit}} = \frac{2}{\pi} \tan^{-1}\left(\frac{|10.1945|}{0.09396}\right) \approx 0.994$. Since $\alpha = 0.9 < \alpha_{\text{crit}}$, the equilibrium remains stable. (For $\alpha > 0.994$, the Matignon condition would be violated, destabilizing E_+.)

Since E_+ and E_- are inherently stable at $\alpha = 0.9$, TDFC is used to test delay robustness whether stability is preserved across the (τ, K) parameter space rather than to suppress chaos.

In what follows, we perform the TDFC-based stability test for the equilibrium E_+ (E_+ and E_- have equal eigenvalues, then they exhibit the same behavior), as can be seen in Figure 7.

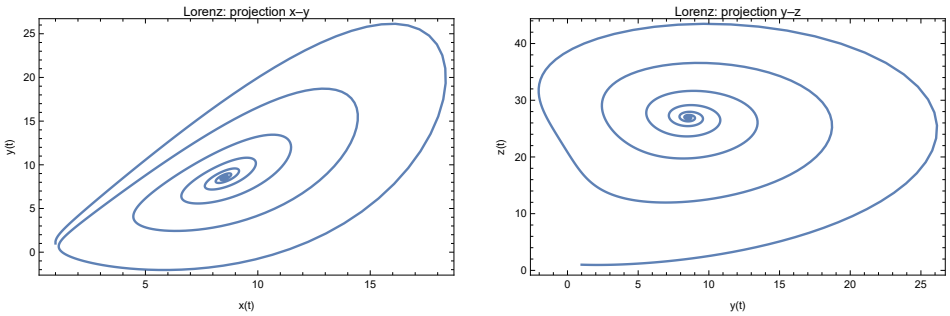


FIGURE 6. Fractional order Lorenz system without delays, for $a = 10$, $b = 8/3$, $c = 28$, $\alpha = 0.9$ and initial conditions $x(0) = 1, y(0) = 1, z(0) = 1$.

The following system is the result of linearization around the equilibrium point $E^* = (x^*, y^*, z^*)$:

$$\begin{aligned} {}^0D_t^\alpha \tilde{x}(t) &= a\left[(\tilde{y}(t) - \tilde{x}(t)\right] \\ {}^0D_t^\alpha \tilde{y}(t) &= (c - z^*)\tilde{x}(t) - x^*\tilde{z}(t) - \tilde{y}(t) + K\left[(\tilde{y}(t-\tau) - \tilde{y}(t)\right] \\ {}^0D_t^\alpha \tilde{z}(t) &= y^*\tilde{x}(t) + x^*\tilde{y}(t) - b\tilde{z}(t) \end{aligned} \tag{3.18}$$

derived from $x(t) = x^* + \tilde{x}(t)$, $y(t) = y^* + \tilde{y}(t)$, and $z(t) = z^* + \tilde{z}(t)$. Here, $\tilde{x}(t)$, $\tilde{y}(t)$, and $\tilde{z}(t)$ are small perturbations around the equilibrium point. By shifting the system (3.16) into perturbation coordinates $\left(\tilde{x}(t), \tilde{y}(t), \tilde{z}(t)\right)$, the equilibrium point E^* is relocated to the origin of the modified coordinate system. The system (3.18) can be written in matrix form as follows:

$$\begin{pmatrix} D_*^\alpha \tilde{x}(t) \\ D_*^\alpha \tilde{y}(t) \\ D_*^\alpha \tilde{z}(t) \end{pmatrix} = \mathbf{J} \cdot \begin{pmatrix} \tilde{x}(t) \\ \tilde{y}(t) \\ \tilde{z}(t) \end{pmatrix} + K \begin{pmatrix} 0 \\ \tilde{y}(t-\tau) - \tilde{y}(t) \\ 0 \end{pmatrix} \tag{3.19}$$

where $\mathbf{J}$ is the Jacobian matrix.

According to Theorem 1, the zero solution of the system (3.19) is asymptotically stable if and only if all the roots s of the characteristic equation:

$$\det[\Delta(s)] = 0 \tag{3.20}$$

have negative real parts, that is, $|\arg(s)| > \frac{\pi}{2}$, where the characteristic matrix $\Delta(s)$ is given by:

$$\Delta(s) = \begin{pmatrix} s^\alpha + a & -a & 0 \\ -(c - z^*) & s^\alpha + 1 + K(1 - e^{-s\tau}) & x^* \\ -y^* & -x^* & s^\alpha + b \end{pmatrix} \tag{3.21}$$

Figure 7 displays the theoretical stability domain of the nontrivial equilibrium E_+ of the fractional Lorenz system under TDFC, obtained from the characteristic equation. The entire rectangular region is uniformly shaded, indicating that for

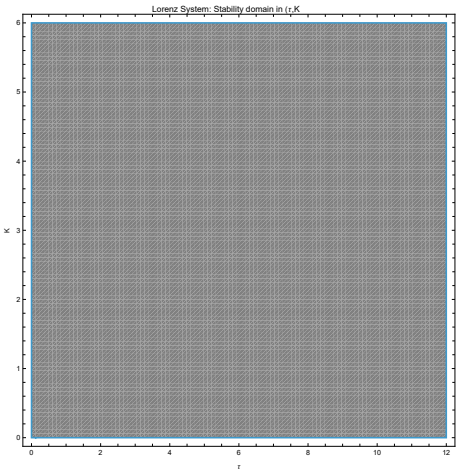


FIGURE 7. Fractional Lorenz system: local stability of E_+ via characteristic equation: shaded area = stable $K \in [0, 6]$ and $\tau \in [0, 12]$.

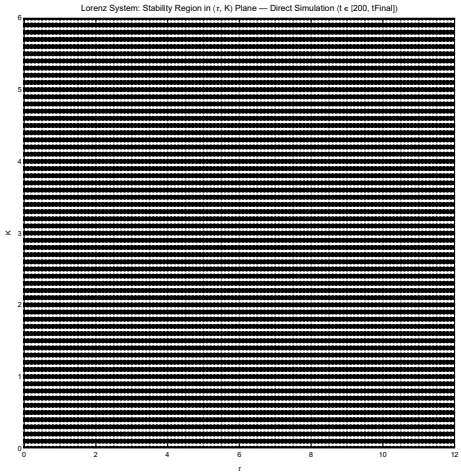


FIGURE 8. Lorenz system (fractional $\alpha = 0.9$) with TDFC: black dots mark (τ, K) stable for $t \geq 200$ with tolerance 10^{-2} under direct simulation.

every tested pair (τ, K), all characteristic roots satisfy the Matignon sector condition (equivalently $\Re(s) < 0$ in the present commensurate case) hence E_+ is stable. In contrast to the Rössler case, where stability appears only in two separated islands, this figure shows no gaps or boundaries inside the scanned parameter window: the equilibrium remains locally stable for delays and gains within the tested ranges ($\tau \in [0, 12], K \in [0, 6]$). This robustness arises from the system's high oscillation frequency, which makes TDFC insensitive to delay variations over this parameter window. However, the characteristic equation (3.20), which contains the transcendental term $e^{-s\tau}$, implies infinitely many roots as τ varies; thus, stability cannot generally be guaranteed for arbitrarily large τ beyond the tested range. Thus, Figure 7 reveals an unusually robust behavior of the fractional Lorenz system, in which the time-delayed feedback method preserves the local stability of E_+ across the entire scanned (τ, K)-domain (delay-robustness). To corroborate the full-domain stability prediction and verify that the stability is preserved in the nonlinear simulations, we performed a numerical simulation using the fractional Forward Euler-Grünwald-Letnikov method in the system (3.16) with the incorporated delay, as shown in the following figures 8, 9 and 10. Figure 8 shows the numerically computed stability map in the (τ, K)-plane: Each black dot marks a delay-gain pair for which the trajectory, starting from $(1, 1, 1)$, remains bounded and satisfies a convergence tolerance of 10^{-2} with respect to E_+ on the tail interval $t \in [200, 300]$. The dots densely fill the entire rectangle, indicating that every sampled (τ, K) is numerically stable and confirms the uniformly shaded theoretical domain in Figure 7. Figures 9 and 10 then illustrate the dynamics for a representative stable pair, here $\tau = 1$ and $K = 0.3$. Figure 9 displays the time

series of $(x(t), y(t)$, and $z(t)$, which exhibit only a short transient before rapidly converging to their equilibrium values and remaining essentially flat for the rest of the simulation window, confirming rapid convergence and robust attraction toward E_+. Figure 10 shows the corresponding three-dimensional trajectory in (x, y, z) space: starting with relatively large outer loops, the orbit spirals inward and condenses into a tight cluster around E_+, providing a geometric visualization of preserved attraction. Taken together, these three figures indicate that the fractional Forward Euler–Grünwald–Letnikov simulations not only corroborate the characteristic equation prediction of full domain stability but also reveal that convergence is uniformly rapid throughout the (τ, K) parameter range.

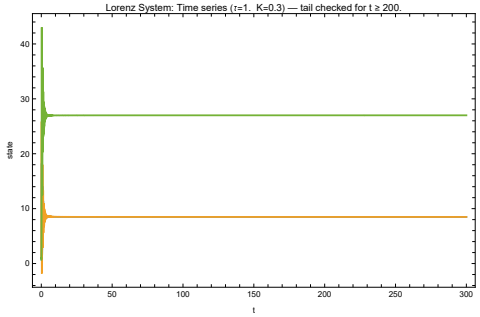


FIGURE 9. The time series plot illustrates the progression of $x(t)$ (blue line), $y(t)$ (orange line), and $z(t)$ (green line) within the fractional-order Lorenz system.

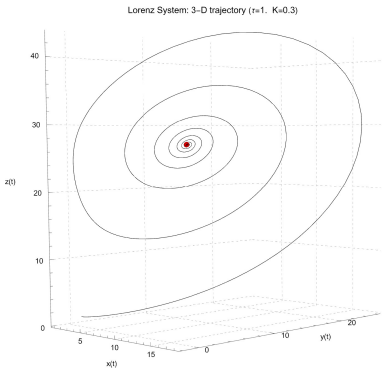


FIGURE 10. The 3D graph of $x(t)$, $y(t)$, and $z(t)$ displays the path of the system converging to a stable area. Starting with chaotic oscillations, the trajectory builds a dense cluster, finally establishing the stabilization of the system.

4. QUANTITATIVE COMPARISON AND ANALYSIS

This stark contrast from the constrained, multi-island structure of Rössler to the universal, globally stable structure of Lorenz exemplifies how system specific dynamical properties determine the effectiveness of a uniform control strategy. As discussed in Section 5, these differences originate in the eigenvalue spectra and architectural couplings of the two systems.

4.1. **Contraction Analysis.** To quantify the discrepancy between the theoretical and numerical stability domains for the fractional Rössler system, we analyze the contraction of the stability set when passing from the characteristic-equation test to the fractional Euler–Grünwald–Letnikov simulations. On the grid $K \in [0, 6]$

Property	Rössler	Lorenz	Interpretation
Fractional order	$\alpha = 0.9$	$\alpha = 0.9$	Common order used in this article
Stabilizable equilibrium	E_- (index-2)	E_+, E_- (index-2, symmetric)	Both have even-index saddles
Unstabilizable equilibrium	E_+ (index-1)	E_0 (index-1)	Odd-number limitation applies
Real eigenvalue λ_1	≈ -9.99	≈ -13.85	Lorenz more stable in real direction
Complex pair: $\Re(\lambda)$	0.199	0.094	Both unstable in spiral plane
Complex pair: $\Im(\lambda)$	0.9797	10.1945	Lorenz 10.4× faster oscillation
Stability domain shape	Two islands	The entire rectangle	Qualitatively different
% grid stable (theory)	35.9%	100%	Full-domain vs. restricted
% grid stable (numerics)	28.9%	100%	Perfect agreement for Lorenz
Theory–numerics agreement	80.5% (19.5% contraction)	100% (no contraction)	Rössler: moderate discrepancy; Lorenz: perfect agreement
Delay sensitivity	High (narrow islands)	Low (full domain)	Frequency-driven robustness

TABLE 1. Rössler vs. Lorenz — Comparative Metrics

with step 0.1 (61 points) and $\tau \in [0, 12]$ with step 0.1 (121 points), we obtain in total 7,381 parameter pairs (τ, K). Among these, the characteristic equation predicts 2,648 stable points, corresponding to 35.9% of the grid, whereas the forward Euler–Grünwald–Letnikov simulations classify only 2,133 points as stable for the chosen tolerance and time window, i.e. 28.9% of the grid. The relative "contraction" of the stability region is therefore:

$$\frac{35.9\% - 28.9\%}{35.9\%} = 19.5\%$$

Agreement (theory–numerics) is 80.5%: 4 of 5 theoretically stable points work in practice; Contraction = 19.5%: 1 of 5 theoretically stable points fail numerically. The characteristic equation is a reliable guide for Rössler, though not perfect. The discrepancy is moderate and concentrated near the bifurcation boundaries. In contrast, Lorenz's 100% agreement shows that the theory is fully sufficient there.

This gap has three main sources. First, the numerical criterion checks convergence only up to $t = 300$, whereas asymptotic stability is defined for $t \mapsto \infty$; near the theoretical stability boundary in the (τ, K)-plane, some characteristic roots s have $\Re(s) \approx 0^-$ (barely satisfying the Matignon criterion), resulting in extremely slow asymptotic decay, and the trajectory may not have entered the ϵ–neighborhood of the equilibrium by $t = 300$, even though it is asymptotically stable. Second, the equilibrium E_- is only locally stable, and its basin of attraction is relatively small for marginal (τ, K); the chaotic initial condition $(0.2, 0.48, 0.731)$ can lie outside this basin, so the simulation diverges from E_- even for parameter values that are linearly stable. Third, the forward Euler–Grünwald–Letnikov scheme introduces discretization errors of order h^α, and the discretization of the delay to multiples of h slightly perturbs the characteristic roots; for points close to the stability boundary, these numerical shifts can move eigenvalues across the imaginary axis and thus destabilize marginally stable cases. In contrast, for the Lorenz system, the dominant real parts are large and negative, implying very fast decay and a large basin of attraction. Then, the direct simulations are much more robust to these effects and produce almost perfect agreement (no observable contraction) between the theoretical and numerical stability regions.

4.2. **Frequency-Robustness Relationship.** This subsection explains why the Lorenz system is robust to delay variations while the Rössler system is sensitive by connecting the natural oscillation frequency of the unstable eigenvalues to the stability domain morphology in the (τ, K)-plane.

For each system, the linearization around the equilibrium yields a complex-conjugate pair of unstable eigenvalues:

$$\lambda_{2,3} = \sigma \pm i\omega_0$$

where: $\sigma = \Re(\lambda)$ is the growth/decay rate (positive means unstable) and $\omega_0 = |\Im(\lambda)|$ is the natural oscillation frequency in radians per time unit. The oscillation period is:

$$T_{osc} = \frac{2\pi}{\omega_0}$$

Now, we calculate frequencies for both systems. For Rössler System (Equilibrium E_-), from the eigenvalue analysis:

$$\lambda_{2,3} = 0.199 \pm 0.9797\, i$$

Natural frequency:

$$\omega_R = 0.9797 \text{ rad/time-unit}$$

Period:

$$T_R = \frac{2\pi}{0.9797} \approx 6.41 \text{ time units}$$

Physical meaning: Without control, perturbations from E_- oscillate with a period of approximately 6.4 time units while slowly growing ($\sigma = 0.199 > 0$).

For the Lorenz system (Equilibrium E_+), from the eigenvalue analysis:

$$\lambda_{2,3} = 0.094 \pm 10.1945\, i$$

Natural frequency:

$$\omega_L = 10.1945 \text{ rad/time-unit}$$

Period:

$$T_L = \frac{2\pi}{10.1945} \approx 0.617 \text{ time units}$$

Physical meaning: Perturbations from E_+ oscillate with a period of approximately 0.62 time units (much faster) while slowly growing ($\sigma = 0.094 > 0$).

Frequency Ratio:

$$\frac{\omega_L}{\omega_R} = \frac{10.1945}{0.9797} \approx 10.4$$

Lorenz oscillates 10.4 times faster than Rössler.

Since $T_R \approx 6.41$ is comparable to the entire delay range , each delay value corresponds to at most two oscillation periods of the Rössler linearization. Small changes in τ therefore produce large changes in the feedback phase and create resonant windows where TDFC works, separated by gaps where it fails. In contrast, $T_L \approx 0.617$ is much smaller than the same delay range, so τ covers almost 20 oscillation periods of the Lorenz linearization. The delayed signal effectively averages over many cycles, making the feedback nearly insensitive to the precise value of τ and producing full-domain stability. Thus, the much larger ω_L explains the strong delay robustness observed for the Lorenz system.

5. Discussion

In this section, we interpret the stability maps obtained for the fractional Rössler and Lorenz systems and compare the analytical predictions with the numerical simulations. The goal is to understand how the combination of fractional order, delay, and feedback gain shapes the performance of TDFC in these two representative chaotic models.

The theory-numeric agreement quantifies how many theoretically stable points are confirmed by direct simulation. For the Rössler system, 80.5% of the 2,648 theoretically stable (τ, K)-pairs are verified numerically, corresponding to a 19.5% contraction. This moderate discrepancy arises primarily near bifurcation boundaries where eigenvalues have small negative real parts, making convergence too slow to satisfy the finite-time criterion ($t \in [200, 300]$, tolerance 10^{-2}). In contrast, the Lorenz system exhibits 100% agreement: every theoretically stable point is numerically confirmed, demonstrating that linear stability analysis is fully sufficient. This difference reflects the Lorenz system's large negative eigenvalues ($\lambda_1 = -13.85$), high-frequency oscillations ($\omega \approx 10.2 rad/TU$), and strong nonlinear coupling, which together ensure rapid convergence even for marginal parameters.

The role of fractional order: In this article, both systems are studied at the common fractional order $\alpha = 0.9$, which simplifies the comparison and isolates the impact of spectral properties and nonlinear coupling. For the Lorenz system, the critical value $\alpha_{crit} \approx 0.994$ derived from condition (3.10) implies that the selected equilibrium changes from unstable ($\alpha > \alpha_{crit}$) to stable ($\alpha < \alpha_{crit}$; at $\alpha = 0.9$ it is

already stable for $K = 0$; thus, TDFC is used to test delay-robustness rather than to suppress chaos. In this setting, the qualitative difference between the two systems, two isolated stability islands for Rössler vs. full-domain stability for Lorenz is not driven by the fractional order itself but by their eigenvalue spectra, in particular the much higher oscillation frequency of the Lorenz complex eigenvalues.

In terms of nonlinear coupling, the two systems behave quite differently. In the fractional Rössler system the z-equation ($z^{\alpha} = b + z(x - c)$) is only weakly coupled to x: the interaction is multiplicative and confined to the third component, so changes in x propagate to z in a relatively localized way. This weak coupling tends to produce a comparatively small basin of attraction around the stabilized equilibrium. In contrast, the Lorenz z-equation ($z^{\alpha} = xy - bz$) contains a strong bilinear xy-term, so both x and y directly drive the evolution of z. The resulting coupling is much stronger and more global, generating a large, highly nonlinear basin that pulls trajectories rapidly toward E_+; together with the strongly negative real parts of the eigenvalues, this helps explain the marked robustness of the Lorenz equilibrium under delayed feedback.

6. CONCLUSION

In this paper, we established a unified framework for analyzing time-delayed feedback control (TDFC) stabilization of fractional-order chaotic systems, with a detailed application to the Rössler and Lorenz systems as representative examples. By combining characteristic-equation analysis based on Matignon's criterion with direct numerical simulation using a compiled fractional Forward Euler–Grünwald–Letnikov scheme, we have mapped the stability regions in the (τ, K)-plane for both systems and clarified the fundamental differences in their response to delayed feedback. The main findings are:

(i) The fractional Rössler system exhibits a two-island stability structure, with stabilization possible only for $\tau \in [0, 4)$ and a narrow band near $\tau \in [8, 11]$, reflecting high sensitivity to delay variations driven by its low frequency eigenvalue spectrum ($\omega_R \approx 0.98 rad/time - unit$).

(ii) The fractional Lorenz system displays full-domain stability across the entire investigated rectangle $K \in [0, 6], \tau \in [0, 12]$, a robustness explained by its high frequency eigenvalues ($\omega_L \approx 10.2 rad/time - unit$) and strong nonlinear coupling, which together render the system insensitive to delay-induced phase detuning.

(iii) Theoretical predictions and numerical simulations agree perfectly for Lorenz (100% correspondence) but show a 19.5% contraction for Rössler, illustrating the practical relevance of finite-time effects, basin of attraction limitations, and discretization errors when designing controllers near bifurcation boundaries.

These results provide both conceptual insight demonstrating that eigenvalue frequency is the primary determinant of delay robustness-and concrete design guidelines: Rössler like systems require careful parameter tuning well inside the stability islands, whereas Lorenz like systems tolerate broad parameter ranges. The methodology developed here serves as a template for the systematic comparative analysis of additional Lorenz-type systems (Chen, Lü, Yang, Liu, Shimizu–

Morioka, and Burke–Shaw) planned for Parts II and III and opens the way for future investigations of α-dependence, multi component feedback, and experimental validation of fractional-order chaos control.

Funding. The authors declare that no funds, grants, or other support were received during the preparation of this manuscript.

Competing interests. The authors have no relevant financial or non-financial interests to disclose.

Author Information. All authors have contributed equally to this work.

Contributions. GM and AG conceived the research idea, FQL conducted the theoretical and numerical analysis, FQL wrote the first draft and prepared the figures, GM and AG supervised the investigation and reviewed the manuscript.

Data availability. The datasets used and/or analysed during the current study are available from the corresponding author on reasonable request.

REFERENCES

[1] I. Podlubny, *Fractional Differential Equations: An Introduction to Fractional Derivatives, Fractional Differential Equations, to Methods of Their Solution and Some of Their Applications*, Academic Press 1st edition, 1999.
[2] C. A Monje, Y. Chen, B. M Vinagre, D. Xue, and V. Feliu, *Fractional-order Systems and Controls: Fundamentals and Applications*, Springer London (2010).
[3] D. Baleanu, K. Diethelm, E. Scalas, and J. J. Trujillo, *FRACTIONAL CALCULUS Models and Numerical Methods*, World Scientific (2012).
[4] I. Petras, *Fractional-order nonlinear systems: modeling, analysis and simulation*, Springer Science & Business Media, 2011.
[5] S. H Strogatz, *Nonlinear dynamics and chaos: with applications to physics, biology, chemistry, and engineering*, CRC press, 2018.
[6] I. Petras, *The fractional-order Lorenz-type systems: A review*, Fractional Calculus and Applied Analysis (2022). https://doi.org/10.1007/s13540-022-00016-4.
[7] A. Gjurchinovski, T. Sandev, and V. Urumov, *Delayed feedback control of fractional-order chaotic systems*, Journal of Physics A: Mathematical and Theoretical, 43(44) IOP Publishing (2010) 445102. https://doi.org/10.1088/1751-8113/43/44/445102.
[8] D. Das, I. Taralova, and J. J. Loiseau, *Time-delay Feedback Control of Fractional Chaotic Rössler Oscillator*, IFAC-PapersOnLine, 58(5) Elsevier (2024) 90–95. https://doi.org/10.1016/j.ifacol.2024.07.069.
[9] E. Lorenz, *Deterministic Nonperiodic Flow*, Journal of Atmospheric Sciences, 20 (1963) 130–148.
[10] O. E. Rössler, *An equation for continuous chaos*, Physics Letters A, 57(5) (1976) 397–398.
[11] M. Nawaz, J. Wei, J. Sheng, A. U. Khan Niazi, and L. Yang, *On the controllability of nonlinear fractional system with control delay*, Hacettepe Journal of Mathematics and Statistics, 49(1) Hacettepe University (2020) 294–302. https://doi.org/10.15672/hujms.546990.
[12] K. Sun, X. I. A. Wang, and J. C. Sprott, *Bifurcations and chaos in fractional-order simplified Lorenz system*, International Journal of Bifurcation and Chaos, 20(04) (2010) 1209–1219. https://doi.org/10.1142/S0218127410026411.
[13] P. Zhou, R. Ding, *Control and synchronization of the fractional-order Lorenz chaotic system via fractional-order derivative* Mathematical Problems in Engineering, 1 (2012) 214169. https://doi.org/10.1155/2012/214169.

[14] K. Pyragas, *Continuous control of chaos by self-controlling feedback* Physics Letters A, 170(6) (1992) 421–428.
[15] D. Matignon, *Stability Results For Fractional Differential Equations With Applications To Control Processing*, 2(03) (1997).
[16] Ch. Li and F. Zeng, *Numerical methods for fractional calculus*, Numerical Methods for Fractional Calculus (2015) 1–280.
[17] M. Xie, S. U. Khan, W. Sumelka, A. M Alamri, and S. A AlQahtani, *Advanced stability analysis of a fractional delay differential system with stochastic phenomena using spectral collocation method*, Scientific Reports, 14(1) Nature Publishing Group UK London (2024) 12047. https://doi.org/10.1038/s41598-024-62851-0.
[18] M. S. Tavazoei and M. Haeri, *A necessary condition for double scroll attractor existence in fractional-order systems*, Physics Letters A, 367(1-2) Elsevier (2007) 102–113. https://doi.org/10.1016/j.physleta.2007.05.081.
[19] H. Nakajima, *On analytical properties of delayed feedback control of chaos*, Physics Letters A, 232(3-4) (1997) 207–210.
[20] F. Q. Lubishtani, Gj. Markoski, and A. Gjurchinovski, *Comparison of numerical and exact solutions of fractional differential equations with constant delay*, Matematichki Bilten- Bulletin Mathématique de la Société des Mathématiciens de la Républikque Macédoine, 48 (1) Faculty of Natural Sciences and Mathematics, Skopje (2024) 53–64. https://doi.org/10.37560/matbil2448153ql.

[1]FERIDE QORROLLI LUBISHTANI
UNIVERSITY OF APPLIED SCIENCE IN FERIZAJ,
FACULTY OF ARCHITECTURE, DESIGN AND WOOD TECHNOLOGY,
FERIZAJ, KOSOVO
Email address: feride.qorrolli@ushaf.net

[2] GJORGJI MARKOSKI
SS. CYRIL AND METHODIUS UNIVERSITY IN SKOPJE,
INSTITUTE OF MATHEMATICS
FACULTY OF NATURAL SCIENCES AND MATHEMATICS,
SKOPJE, NORTH MACEDONIA
Email address: gorgim@pmf.ukim.mk

[3] ALEKSANDAR GJURCHINOVSKI
SS. CYRIL AND METHODIUS UNIVERSITY IN SKOPJE,
INSTITUTE OF PHYSICS
FACULTY OF NATURAL SCIENCES AND MATHEMATICS,
SKOPJE, NORTH MACEDONIA
Email address: agjurcin@pmf.ukim.mk

Received 15.03.2026
Revised 03.06.2026
Accepted 04.06.2026